



HAL
open science

Investigation of caesium retention by potassium nickel hexacyanoferrate (II) in different pH conditions and potential effect on the selection of storage matrix

Isabelle Martin, Cédric Patapy, Cedric Boher, Martin Cyr

► To cite this version:

Isabelle Martin, Cédric Patapy, Cedric Boher, Martin Cyr. Investigation of caesium retention by potassium nickel hexacyanoferrate (II) in different pH conditions and potential effect on the selection of storage matrix. *Journal of Nuclear Materials*, 2019, 526, pp.151764. 10.1016/j.jnucmat.2019.151764 . hal-02428595

HAL Id: hal-02428595

<https://hal.insa-toulouse.fr/hal-02428595>

Submitted on 20 Dec 2021

HAL is a multi-disciplinary open access archive for the deposit and dissemination of scientific research documents, whether they are published or not. The documents may come from teaching and research institutions in France or abroad, or from public or private research centers.

L'archive ouverte pluridisciplinaire **HAL**, est destinée au dépôt et à la diffusion de documents scientifiques de niveau recherche, publiés ou non, émanant des établissements d'enseignement et de recherche français ou étrangers, des laboratoires publics ou privés.



Distributed under a Creative Commons Attribution - NonCommercial 4.0 International License

Investigation of caesium retention by potassium nickel hexacyanoferrate (II) in different pH conditions and potential effect on the selection of storage matrix.

Isabelle Martin^a, Cédric Patapy^{a*}, Cédric Boher^b and Martin Cyr^{a*}

^a LMDC, Université de Toulouse, INSA, UPS, 135 Avenue de Rangueil, 31077 Toulouse, France

^b Orano Projets–Hall de Recherche de Beaumont, 25 avenue de Tourville –BP38, 50120 Equeurdreville, France.

Abstract

The chemical stability and caesium retention properties of a nonstoichiometric compound $K_{2-x}Ni_{x/2}[NiFe(CN)_6].nH_2O$ (KNiFCN) was studied in different pH conditions. Different solutions with controlled pH were prepared. Leaching tests were done with chemical analysis of the solutions. The compound was characterized before and after exposure by chemical analysis, SEM-BSE, X-ray diffraction and infrared spectroscopy. The face-centered cubic (FCC) structure of KNiFCN without caesium was stable even in presence of 1 g/l HNO_3 (pH equal 2) or NaOH (pH equal 13). In presence of caesium trapped on KNiFCN structure, it appears that the increase in caesium content change the KNiFCN structure, thus influencing the retention properties in KNiFCN according to the pH of the solution. The KNiFCN structure was decomposed when the NaOH concentration exceeds 1 g/l (pH equal 14), probably due to the hydrolysis of constitutional elements. A selection of cementitious matrix is the proposed to satisfy stability conditions of this compound.

Keywords : nuclear waste solution, pH value, chemical stability, potassium nickel hexacyanoferrate (II), caesium (noticed Cs).

1 Introduction

Large volume of radioactive liquid waste are produced worldwide from uranium ore treatment or after contact with solid radioactive elements in nuclear power plants. Recently accidental situations can also be at the origin of massive amounts of liquid wastes as it has been the case

with the flood occurring in Fukushima power plant in 2011. Depending on the origin of these wastes, different radioactive elements can be found like uranium (^{238}U), americium (^{241}Am), plutonium (^{240}Pu , ^{239}Pu , ^{238}Pu), neptunium (^{237}Np). Gamma radiations which are hazardous are emitted for instance by Cobalt (^{60}Co), Strontium(^{90}Sr) and Caesium (^{137}Cs).

Drastic reduction of hazardous elements concentrations in effluents can be acquired through different process with the most used being co-precipitation ([1]–[6]). This processing operation consists in introducing chemical reagents to the wastewater to form insoluble salts which could be then confined in a solid matrix for long term storage [1], [7]. This effluent treatment involves a complex mechanism of ion exchange and chemical adsorption to permit the radionuclide trapping. The selection of trapping sorbent depends on the type of radionuclide present in the wastewater but also on the volume of effluent to be treated in order to optimize the cost of the process. ^{137}Cs is one of the most prevalent radionuclide where zeolites, tetraphenylborate and especially cyanoferrates sorbents are used to get the selective insolubility of caesium.

Transition metal hexacyanoferrates (II) are added at one step of the treatment of effluents with pH adjustment to allow the trapping of caesium inside insoluble salts [8], [9]. For example, the compound of interest in this study is obtained by the in-situ reaction of hexacyanoferrate with nickel sulfate to form a nickel hexacyanoferrate II (Ni-Fe^{II}). Its structure is based on six cyanure groups (CN) organized in an octahedral configuration with Fe-CN-Ni-NC-Fe bounds between them to form a face-centred cubic cell. Electroneutrality is maintained by potassium cations in interstitial sites. An exchange mechanism between K^+ and Cs^+ will be at the origin of caesium trapping. A ratio Ni/Fe of 1-1.5 was shown to be efficient to optimize exchange between caesium (noticed Cs) and potassium in solutions ([1], [10]). Different authors suggest that sorption capacity depends also on the temperature [11] and on the concentration of Cs in the solution but no data is available to confirm it [12].

The addition of nickel sulfate to form the nickel hexacyanoferrate can lead to high value of pH (10.4-11.7) which is then corrected to favor the insolubility of salts containing Cs. Moreover, the radioactive waste encapsulation is often realized by confinement of the insoluble salts (with residual water) in a solid matrix which can be composed of liquid exhibiting basic conditions (high pH values) up to 13 [11]. Some data are available for potassium/nickel hexacyanoferrate II ($\text{K-Ni-Fe}^{\text{II}}$) in the literature ([9], [11]). This compound is closed to the nickel hexacyanoferrate with lower Ni/K ratios ($\text{K}_{0.87}\text{Ni}_{1.57}\text{Fe}(\text{CN})_6$). It was exposed in [9], [11] to solutions with different concentrations of HCl, HNO_3 and NaOH to reach different pH

up to 14. X-Ray diffraction patterns coupled with quantification of Fe in the solution (ICP-OES) showed a degradation of the compound for pH between 13 and 14. On the contrary, no significant degradation of the K-Ni-Fe^{II} was observed in acidic conditions. The ability of retention of Cs was constant up to pH = 13 with a dramatic decrease above.

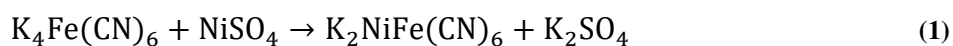
It is then practically of prime importance to understand the influence of the pH conditions on the ability of Ni-Fe^{II} to keep Cs elements inside its structure. This information can be used to correctly select the operating conditions (time of mixing, concentrations of reactive compounds for pH adjustment,...) and appropriate coating matrix ensuring containment of the radioactive waste without radionuclide release.

The present study deals with the influence of the pH of the solution on the Cs retention properties in Ni-Fe^{II} in order to determine a appropriate cement matrix of radioactive waste encapsulation. The sorbent will be first exposed to three different Cs concentrations to obtain different exchange level inside the structure. It will then be exposed to different pH between 2 and 14 using HNO₃ and NaOH. The solutions will be characterized by ICP-OES and ion chromatography to both measure the potential release of Cs and the degradation of the sorbent. X-Ray diffraction (XRD), FTIR and chemical analysis done by SEM-EDS will be used to identify transformation of the sorbent after exposure.

2 Experimental set-up

2.1 Preparation and stoichiometry of potassium nickel hexacyanoferrate (II).

A nonstoichiometric compound K_{2-x}Ni_{x/2}[NiFe(CN)₆].nH₂O (KNiFCN) has been prepared by reaction between potassium hexacyanoferrate (II) (K₄Fe(CN)₆.3H₂O) and nickel sulphate hydrate (NiSO₄.6H₂O), according to equation (1).



The two reactants were introduced in molar ratio [Ni]/[Fe(CN)₆] equal to 1.22. The average chemical composition was estimated as K_{1,96}Ni_{1,22}Fe(CN)₆ by the quantification of Ni, Fe and K elements by Atomic Absorption Spectrometry (PERKIN ELMET AAnalyst 400). Particle size distributions obtained by laser granulometry (CILAS/1090 LD model) were D₉₀ = 4.2 μm, D₅₀ = 1.7 μm and D₁₀ = 0.3 μm.

2.2 Simulation of Cs trapping

Caesium nitrate (CsNO_3 99.8%, Alfa Aesar) was added to the solution to simulate the Cs present without radiological toxicity. Table 1 shows the four concentrations of Cs in the simulated solutions used for the study. Haas [13] showed that quantity of Cs trapped inside nickel potassium hexacyanoferrate are generally comprised between 350 and 1900 mmol Cs/g of the sorbent. Then, the highest concentration of Cs in the study (2000 mmol Cs/g) may correspond to a situation of the maximum capacity of fixation of the hexacyanoferrate. Potassium nickel hexacyanoferrate (II) was added to the simulated solutions (total volume = 1 l) and mixed at ambient temperature during 24 hours to ensure that Cs is trapped into the KNiFCN.

Table 1: Concentration of Cs in the simulated solutions.

	Control solution	Solution I	Solution II	Solution III
[Cs] (mol/mol Fe)	0	$3.3 \cdot 10^{-1}$	$2.9 \cdot 10^1$	$2.0 \cdot 10^3$

$V = 100 \text{ ml}$ and $19 < [\text{KNiFCN}] \text{ (g/l)} < 25$

2.3 Exposure to different pH

The chemical stability was studied by exposing the simulated solutions to either HNO_3 and NaOH (analytical grade) solution in the range of 0.03 to 50.0 g/l at 20°C for 1 day (Table 2). It can be noticed that the reference pH of the compound in solution is 8. Experiments were done in 100 ml PE containers with stirring using an end-over-end agitator for 24h at 20°C . After mixing, the simulated solutions containment KNiFCN were filtered with $0.45 \mu\text{m}$ filter and diluted by 2% of HNO_3 addition. Acidification prevents precipitation of stable phases. At the end, the solution was stored in plastic vial at 5°C to avoid any precipitation of solid before analysis. The solution concentrations of Cs, Fe and Ni were analysed by ICP-OES (Optima 7000DV-Perkin Elmer), Atomic Absorption Spectrometry (Aanalyst 400-Perkin Elmer) and ionic chromatography (ICS 3000-Dionex). The residual solid phase after testing was isolated by drying at 20°C for 1 day before crushing into fine powder ($< 80 \mu\text{m}$) for microstructural characterisation. X-Ray diffraction analyses were done with a Siemens D5000 ($\text{CoK}\alpha$, $\lambda = 1.789 \text{ \AA}$) working in Bragg-Brentano geometry with a 2θ range of 5° - 70° . Lattices parameters were determined with Fullprof software. The solid phase was also analysed by Fourier transform infrared spectroscopy method (FTIR, Perkin-Elmer Spectrum). The analysis

was made by deposition of a low amount of powder directly on the diamond cell after measurement of the background in air medium. The spectrum obtained was an accumulation of 10 measurements made between 4000 cm^{-1} and 800 cm^{-1} . For SEM observations, the samples were pressed until 75 MPa during 2 min to obtain pellets of 4–5 mm thickness. The pellets were impregnated under vacuum with an epoxy resin (MECAPREX MA2+) and polished with different polishing pads and diamond spray ranging from 12 to 1 μm .

Table 2: Concentration of HNO_3 and NaOH used for chemical stability studies.

Notation	pH2	pH8_reference	pH10	pH11	pH12	pH13	pH14
pH	2	8	10	11	12	13	14
$[\text{HNO}_3/\text{NaOH}]$ (g/l)	1.22	0.0	0.06	0.13	0.03	1.03	5.08

3 Results and discussion

3.1 Influence of Cs concentrations in the solution on the reference product

The potassium nickel hexacyanoferrate product was exposed to different concentrations of Cs (dissolution of caesium nitrate) to reach different quantity of Cs trapped inside the Ni-Fe^{II} sorbent. It will be seen - as discussed later in the paper - (Figure 4) that the concentration of Cs in the solution is very low after the process of fixation by the hexacyanoferrate whatever the initial concentration of Cs in the solution.

Figure 1 presents SEM-BSE observations of residual solid obtained after exposure of the nickel hexacyanoferrate to different concentrations of Cs (0, 0.3, 30 and 2000 mmol/mmol Fe). The BSE mode of the SEM highlighted different grey levels corresponding to heterogeneous atomic numbers (Z). This was slightly visible for Ni-Fe^{II} compounds exposed to low concentrations of Cs (0 and 0,3 mM). The presence of some cracks may be due to the sample preparation (polishing and vacuum stage in the SEM). Elements ratios (Fe/Ni vs K/Ni) obtained by EDS analysis (50 points) are plotted in Figure 2. The high level of dispersion of the chemical compositions seems to show that the composition of KNiFCN was heterogeneous (Fe/Ni between 0.7 and 1.1 and K/Ni between 1.1 and 2.4 for the Ni-Fe^{II} exposed to 0.3 mM for example). The spread is more pronounced under variations of K/Ni ratios depending on the localization of the pointing. As K^+ ions are replaced by Cs^+ ones during the co-precipitation process, heterogeneities may appear in the Ni-Fe^{II} depending on

the spatial distribution of the Cs. The higher the Cs is trapped inside the structure, the lower the K/Ni is. This was confirmed by the narrowing of the heterogeneities of K/Ni ratios for the sample with the highest Cs concentration (K/Ni between 0.6 and 1.2). Fe/Ni ratio are roughly similar whatever the initial concentration of Cs of the solution. Thereafter, plots indicated that the addition of a low amount of Cs (0.3 mM) did not clearly change the chemical composition of KNiFCN. However, the cloud of EDS analyses points moves toward a lower values of K/Ni ratio for the highest amount of Cs (2000 mM). Finally, it is interesting to note that the presence of K^+ in the sorbent means that the K^+ ions substitution by Cs^+ ions was not complete. This is in accordance with the work of Ravat [12] which revealed that no more than 22% of the K^+ can be substituted by Cs. It is possible that higher contents of Cs could be trapped by substitution of K^+ by Cs^+ .

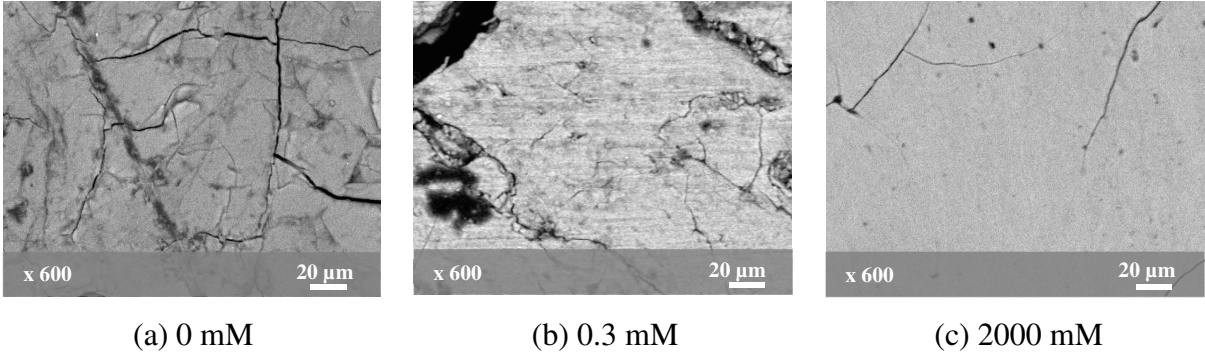


Figure 1: SEM-BSE images of nickel hexacyanoferrates powder (solid residual) after exposure to different Cs concentrations samples at pH equal 8.

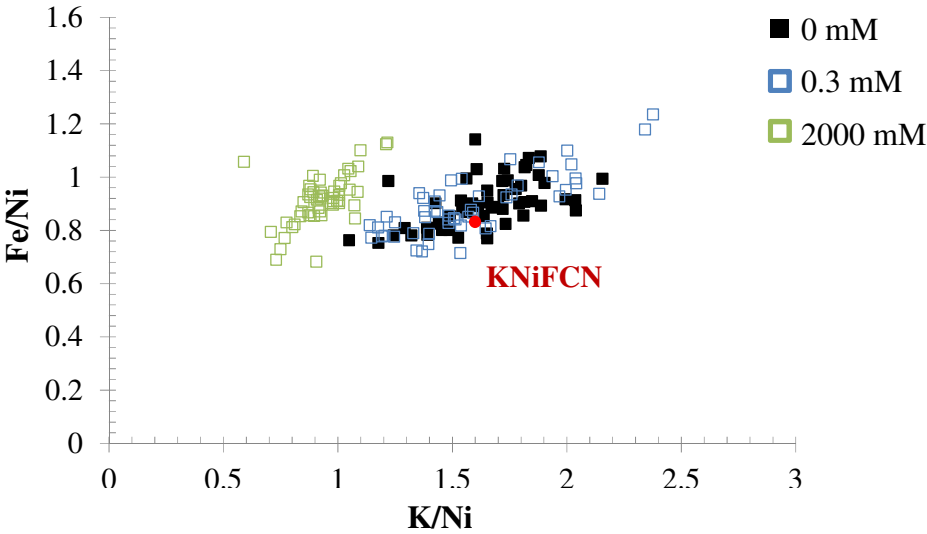


Figure 2: EDS analysis (50 points) of KNiFCN-Cs samples presented in figure 1 for 0, 0.3 and 2000 mM of Cs.

Figure 3 shows XRD patterns of the Ni-Fe^{II} samples exposed to 0, 0.3, 30 and 2000 mM of Cs. These diagrams were very similar to the ones obtained by Gelling [14]. They confirmed the presence of the crystalline phase of nickel/ potassium ferrocyanure (K₂NiFe(CN)₆) with a face-centered cubic (FCC) cristalline structure (database code ICSD 28667). On another hand, these investigations permit to confirm a change in the crystal structure in identifying a left shift of peaks for higher amounts of Cs inside the structure (30 and 2000 mM). According to some authors ([11], [15]), Ni and Fe elements are located at the corners of the elementary cubic lattices, cyano groups (CN) on the edges and the exchangeable cations (K⁺ and Ni²⁺) at the body center. When K⁺ ions (atomic radius (R_{atomic}) = 2.77 Å) are replaced by Cs⁺ ions (R_{atomic} = 3.34 Å), a lattice parameter modification (a, Å) can be observed with a shift to the left of the peak corresponding to larger lattice parameters. XRD patterns were simulated with Fullprof software to evaluate the modification of the “a” lattice parameters (see Table 3). A larger “a” dimension is obtained with increasing Cs concentrations might indicate replacement of K⁺ by Cs⁺.

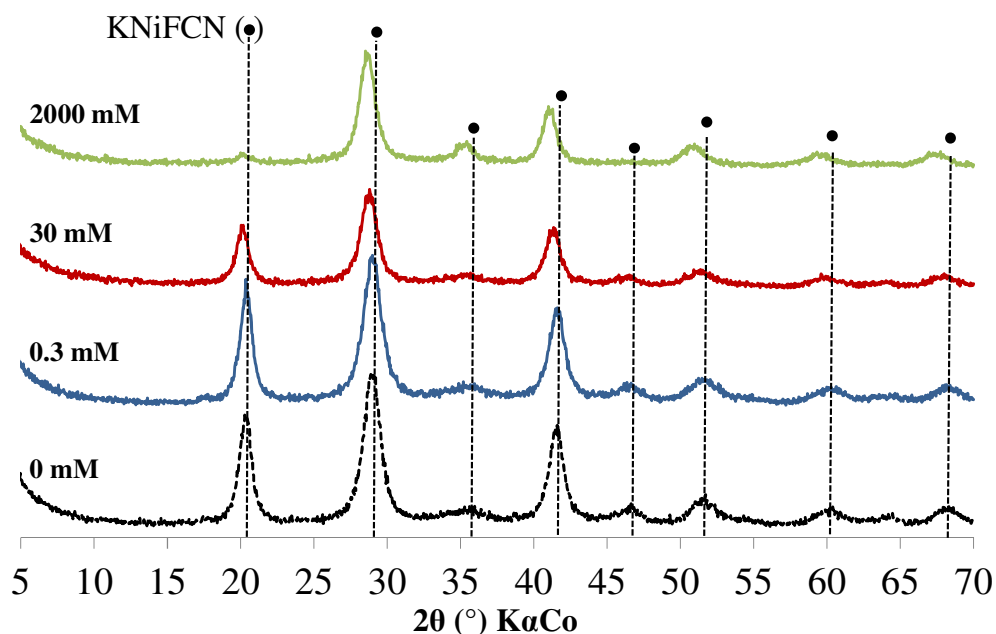


Figure 3: XRD diffractograms of different KNiFCN-Cs products at pH equal 8.

Table 3: Lattice parameter (a) for the different KNiFCN-Cs samples at pH equal 8.

	a (Å)
0 mM	10.050
0.3 mM	10.055
30 mM	10.062
2000 mM	10.167

3.2 Behaviour of KNiFCN under different pH conditions

3.2.1 Evolution of the Cs trapping capacity of KNiFCN-Cs systems as a function of the pH of the solution

The Cs capacity was evaluated by doing quantification of Cs⁺ of the solution in contact with KNiFCN during expositions in solution.

As presented above, reference experiment were done with KNiFCN exposed at pH=8 (equilibrium pH) to evaluate the distribution between Cs in liquid and Cs trapped inside the KNiFCN structure. To compare leaching of Cs⁺ at different pH levels, concentrations were presented in Figure 4 on a percentage basis of the reference (Cs⁺) in solution at pH=8 for a given initial concentration of Cs (0.3, 30 or 2000 mM).

A negative percentage in Cs⁺ ions proportions indicates a potentiel reuptake by KNiFCN or a trap throughout the other phases precipitation and a positive percentage shows potential Cs leaching initially trap in KNiFCN-Cs products. The error associated to these measurements is about 2%. Likewise trends indicate that the initial Cs concentration introduced in the solution influences the chemical stability of KNiFCN-Cs products. In the case of low Cs concentration (0.3 mM), the proportion of Cs dissolved increases gradually over the pH values range from 8 to 12. In acid condition, the proportion of Cs dissolved reach in total the value of 5%, equal to a solution at pH equal 13. In high alkaline solution (pH equal 14), the proportion of Cs dissolved strongly increased to reach the value of 15%. This high proportion of Cs dissolved indicate a potential downgrading and/or restructuring KNiFCN-Cs products. Further investigations were carried out on the solid phases to give more information over this downgrading/restructuring phenomena (see part 3.2).

The increase in Cs concentration sorbed, until an intermediate concentration (30 mM) leads to a modification of a KNiFCN-Cs product downgrading phenomena. In fact, in light of the results presented in Figure 4, it appears that the Cs dissolved content in the solution is very low (< 0,1%) and constant until over whole pH range tested. However, in the case of Solution

III (2000 mM), a change of the proportion of Cs⁺ ions is observed in the solution. In acid condition, a lack of Cs in solution is observed. Then a decrease of Cs proportion is observed when the pH of the solution increased from 8 (pH reference) to 11. This increase seems to show a reuptake by KNiFCN product (optimal pH condition where the Cs⁺ ions sorption is optimised) or by a news products precipitation. The change of the proportion of Cs⁺ ions could be due to a competition between dissolved Cs (chemisorption) and reuptake Cs (physisorption). At pH equal 13 the proportion of Cs⁺ ions in solution achieve 6%. Then this proportion value drop down at pH equal 14. The global evolution of Cs⁺ ions in solution with pH for solution III (2000 mM)) was not completely explained and these measurements should be repeated to confirm this trend.

The overall results show that, at high pH and especially for low Cs concentration of the solution, the amount of Cs released can be significant, notably if the adsorbant (KNiFCN) is stocked in porous matrix allowing the radionucleides diffusion.

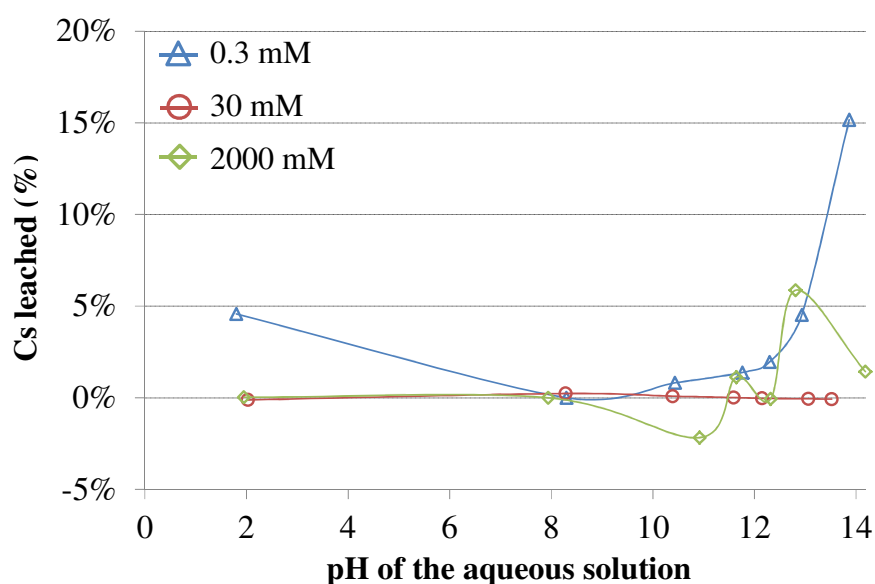


Figure 4: Dissolution percentage of Cs from KNiFCN-Cs at different pH values of the aqueous solution*

* Cs leached corresponded to the ratio between initial Cs concentration in solution for a pH equal 8 (pH8_ref) and the Cs concentration in solution at different pH.

3.2.2 Characterization of the solid products after exposure to different pH values of the aqueous solution.

(a) Control solution (0 mM of Cs)

In order to identify and follow the evolution of KNiFCN within the KNiFCN-Cs systems, FTIR spectroscopy was used. Figure 5 (a) shows the different spectra of the control solution between 4000 cm^{-1} and 1200 cm^{-1} , after chemical treatment at 20°C . On these spectra, six major vibrations bands were identified:

- $1385\text{-}1410\text{ cm}^{-1}$: may be due to the presence of CO_3^{2-} anions due to carbonation of $\text{Ni}(\text{OH})_2$ (interaction with air) [16] and shows the presence of nitrate group [17].
- $1420\text{-}1450\text{ cm}^{-1}$: could be due to the presence of HCO_3^{2-} anions [40], probably due due to carbonation of $\text{Ni}(\text{OH})_2$.
- 1640 cm^{-1} : associated with bonding vibrations of H-OH bonds, related to water [39].
- $2085\text{-}2100\text{ cm}^{-1}$: corresponding to the stretching vibration of CN bonds in the ferrocyanure group ($\text{Fe}(\text{CN})_6^{3-}$) [15].
- 3400 cm^{-1} : arises from O-H stretching vibration of water molecules [18] [39].
- 3640 cm^{-1} : could be due to the O-H stretching vibrations, related mainly to $\text{Ni}(\text{OH})_2$ [16] [19].

Figure 5 (b) presents the characteristic bands of the CN group (between 2200 cm^{-1} and 1900 cm^{-1}) for the control solution after chemical treatment (acid condition - left spectrums, and basic conditions - right spectrums) at 20°C . First, it is noted that the decrease or the increase of the pH values of the solution, until 13 did not affect the chemical environment of the ferrocyanure compound (no shift of the vibration bands). Under acid condition, a decrease in the intensities of the ferrocyanure compound was observed. Similarly, under basic conditions, a gradual decrease in the intensities of the CN bonds vibration over a range of pH values up to 11 was noted. The decrease in the intensities of this vibration mode suggests a probable downgrading of the KNiFCN product. Conversely, above 12, an increase in intensities is observed, reflecting a precipitation or restructuring KNiFCN-Cs products. Beyond the pH value of 12 a new downgrading is observed and even a total disappearance for a extreme pH value (pH equal 14), accompanied by the change of the position of the cyano stretch (from 2085 cm^{-1} to 2038 cm^{-1}) and the nickel hydroxide precipitation (see Figure 5

(a). The vibration bands shift to lower wavelength values, inferring the change in the oxidation state of FeII [20].

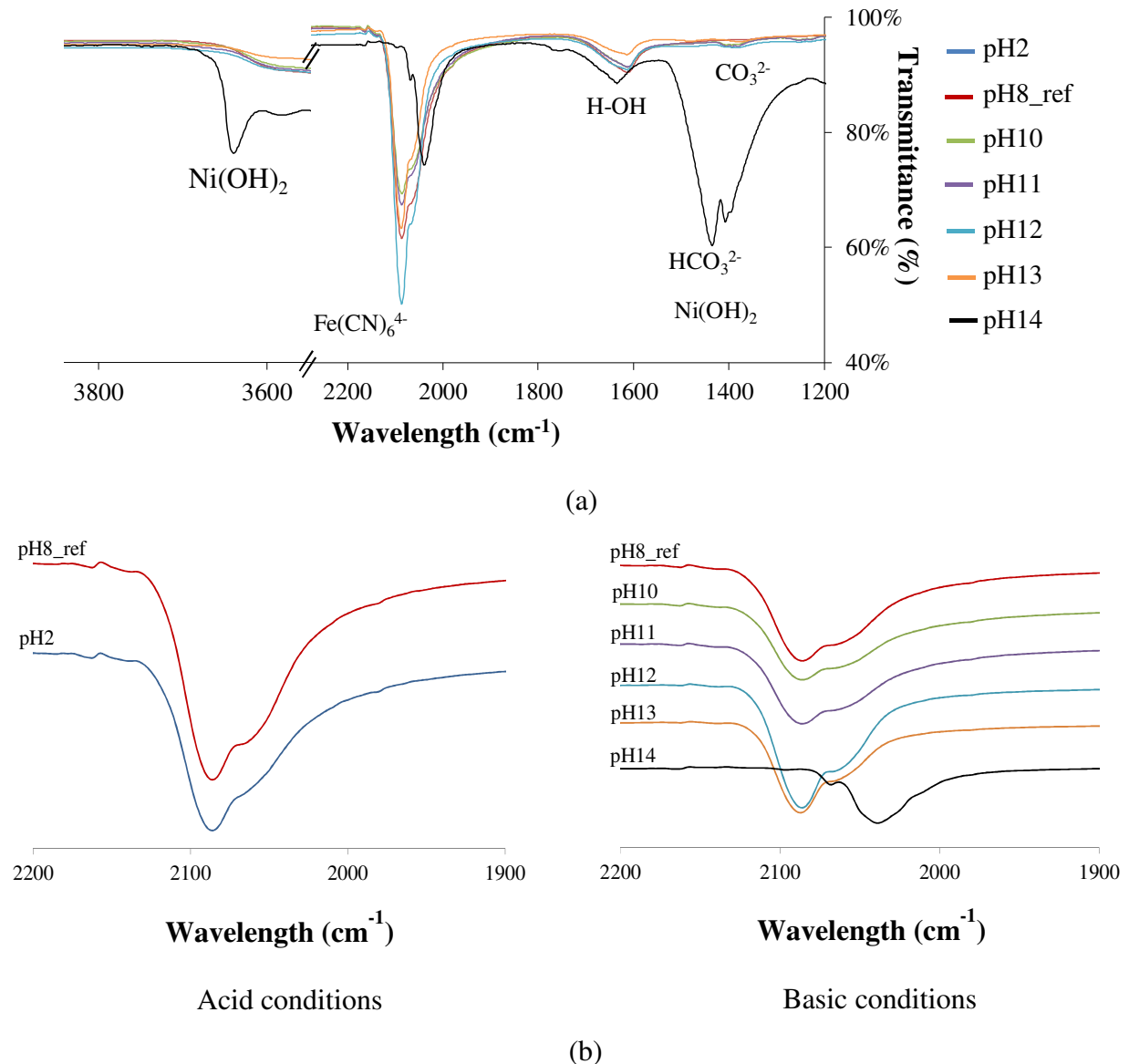


Figure 5: FTIR spectra of Control solution (0 mM of Cs) for different pH values of aqueous solution (a) and zooming a section of FTIR spectra around bonding vibrations of KNiFCN products (b).

Further investigations realized by XRD (Figure 6) and SEM-EDS (Figure 8) confirm the previous observations by showing the nickel oxide (noted N on Figure 6) and iron hydroxide (noted F on Figure 6) formation when the pH value of the solution equal 14. Then the XRD analyses present in Figure 6 (a) show the presence of a secondary phase: nickel ferrocyanure (Ni₂Fe(CN)₆). The ferrocyanure downgrading leads to a loss of the system crystallinity (strong presence of amorphous product). Figure 6 (b) shows the effect of treatment

concentration of HNO₃ and NaOH on the lattice parameter (a) of the KNiFCN sample for solution without Cs (Control solution – 0mM of Cs). The ‘a’ value for the sample treated with HNO₃

(pH 2) and NaOH (pH 10 to pH 13) is in the range of 10.048 to 10.056, which is close to that for the original sample (pH 8_ref). The KNiFCN damage observed when the concentration of NaOH is high, does not allow the lattice parameter determination.

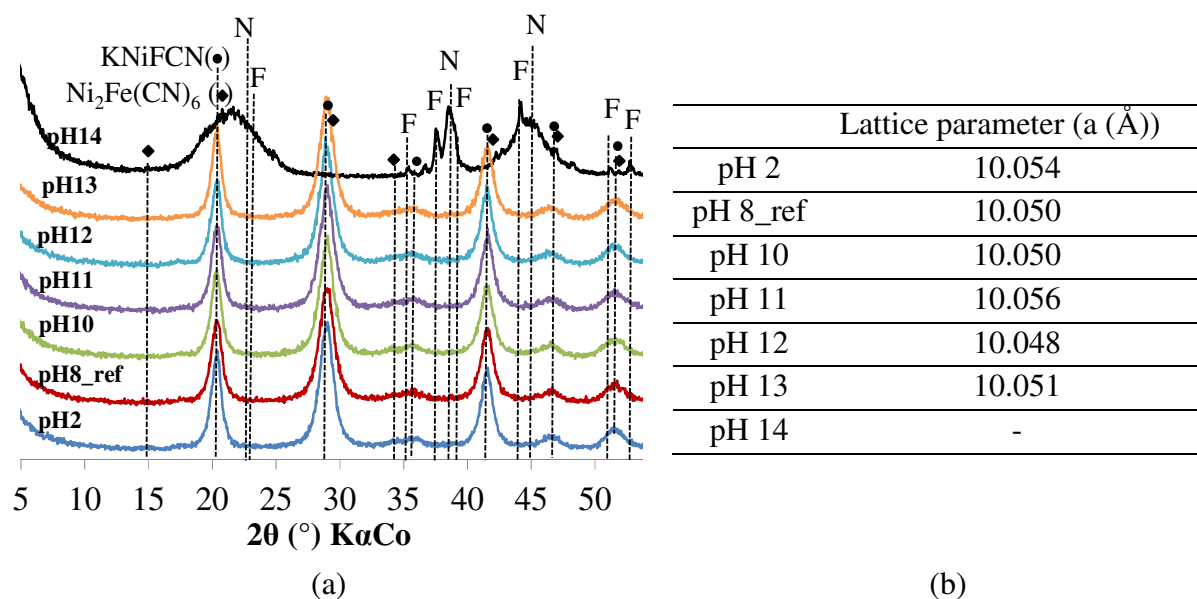
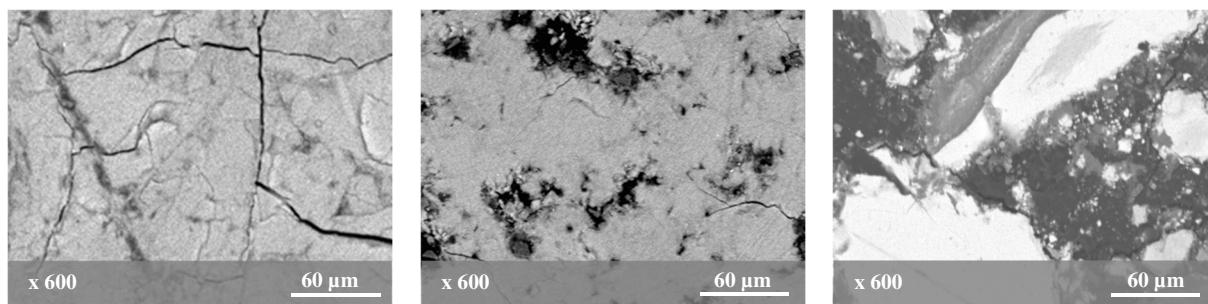


Figure 6: XRD analyses of the Control solution (0 mM of Cs) after different chemical treatment (a) and lattice parameter according to the pH values of the aqueous solution (b) with N:NiO and F:Fe(OH)₂.

The microstructure of the KNiFCN product at different pH of the solution are shown in Figure 7. The lack of grey nuance for KNiFCN product at pH equal 8 (Figure 7 (a)) and 12 (Figure 7 (b)) illustrate a homogeneous chemical composition. However, when the pH of the solution increase to 14, the chemical composition becomes heterogeneous (see Figure 7 (c)) with the presence of nickel hydroxide (white grain) and a rich sodium compound (light grey grain). EDS analyses done on 50 points in the KNiFCN product at different pH (Figure 8) show a clear evolution from KNiFCN compound to Ni(OH)₂ and Fe(OH)₂ at pH-value of 8 to 14.



(a) pH8_ref (b) pH12 (c) pH14

Figure 7: SEM-BSE images of KNiFCN product at pH equal 8, 12 and 14.

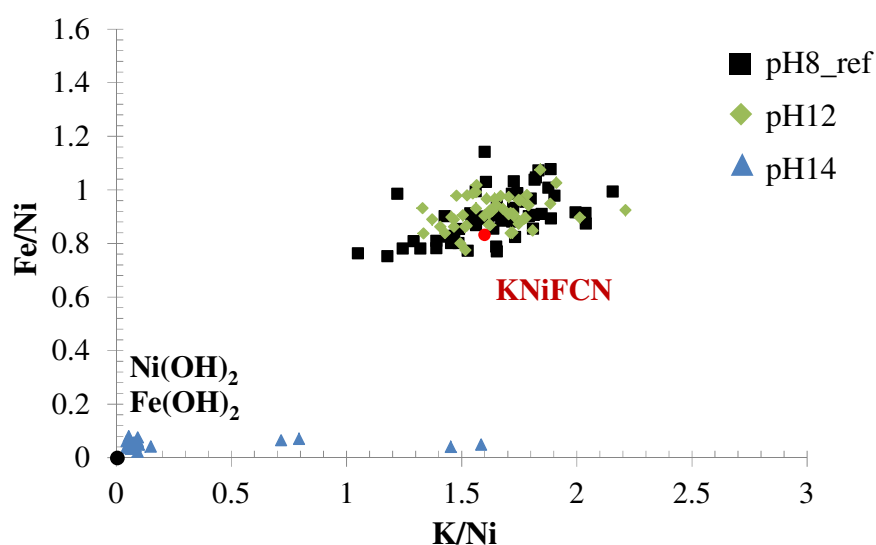


Figure 8: SEM-EDS analysis of KNiFCN product at pH equal 8, 12 and 14.

(b) Solution I (0.3 mM of Cs)

Figure 9 shows the different spectra of the Solution I (0.3 mM of Cs) after a treatment at different pH at 20°C. The addition of Cs in KNiFCN structure leads to the precipitation of one or more new compounds, not observed by X-ray diffraction (Figure 10 (a)). The characteristic bands of these new compounds are present at 1250 cm⁻¹ and 1230 cm⁻¹ (double vibration bands) identified as:

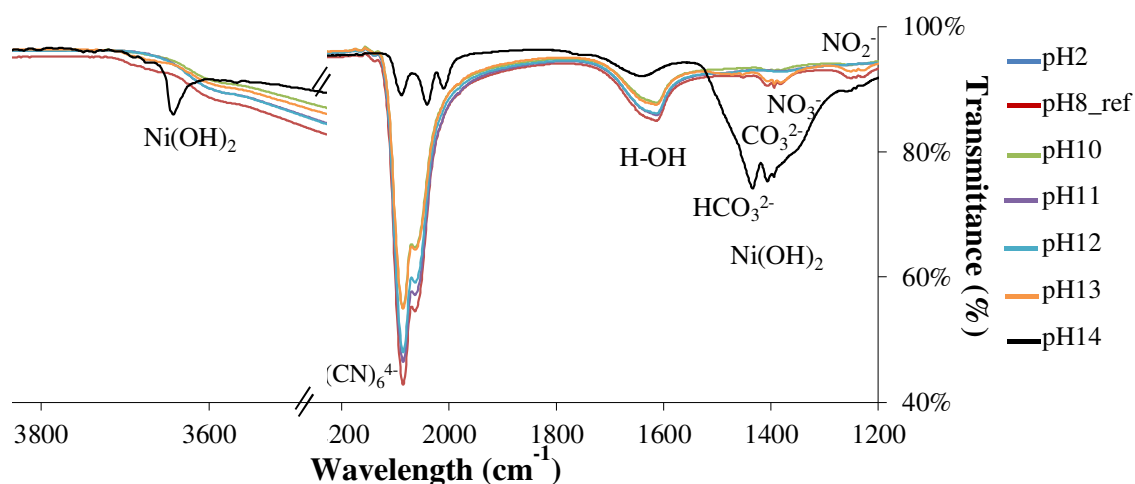
- 1230-1260 cm⁻¹: may be due to the presence of NO₂⁻ anions [17] [40] associated to the insertion of Cs nitrate in solution (0.3 mM of CsNO₃).

The non-detection of the nitrate group by X-ray diffraction seems to suggest a loss in their crystallinity or their low concentration.

For the acid condition (Figure 9 (b) (left spectrums)), the intensities of the ferrocyanure compound are not modified. However, according to the previous results, 5% of Cs is detected in solution (Figure 4). Two theories can be used to explain this Cs presence in solution:

- Cs desorption: references found in the literature show that the KNiFCN is more effective for the removal of Cs^+ from highly concentrated solutions of Na^+ (from NaOH in solution) and H^+ (from HNO_3 or HCl in solution) [11], [21].
- Downgrading of the news compounds observed at pH equal to 8 (Figure 9 (b)).

In basic condition (Figure 9 (b) (right spectrums)), an important decrease in the intensity of stretching vibration of CN is observed when the pH of the solution increases from 8 to 10. However, the lack of Cs in solution (see Figure 4) indicates that Cs remains trapped in the solid phase, despite the possible KNiFCN downgrading. A less important decrease in the intensity of ferrocyanure's vibration is observed for pH solution at 11 (violet curve) and 12 (blue curve). A less important decrease in the intensity of ferrocyanure's vibration is observed for pH solution at 11 (violet curve) and 12 (blue curve) without Cs discharge (see Figure 4). When the pH of the solution increases from 8 to 13 (orange curve), the important decrease in the intensities of ferrocyanure's vibration is correlated to the presence of Cs in solution (5% of Cs detected in solution, see Figure 4). Finally, a new behavior is observed when the pH of the solution reaches a value of 14 (black curve). Infact, a strong decrease in the intensity of ferrocyanure's vibration coupled to the emergence of news vibrations bands at 2047cm^{-1} and 2010cm^{-1} reflects the chemical environment changing of ferrocyanure, leading to the loss of its sorption capacity (15% of Cs detected in solution, see Figure 4).



(a)

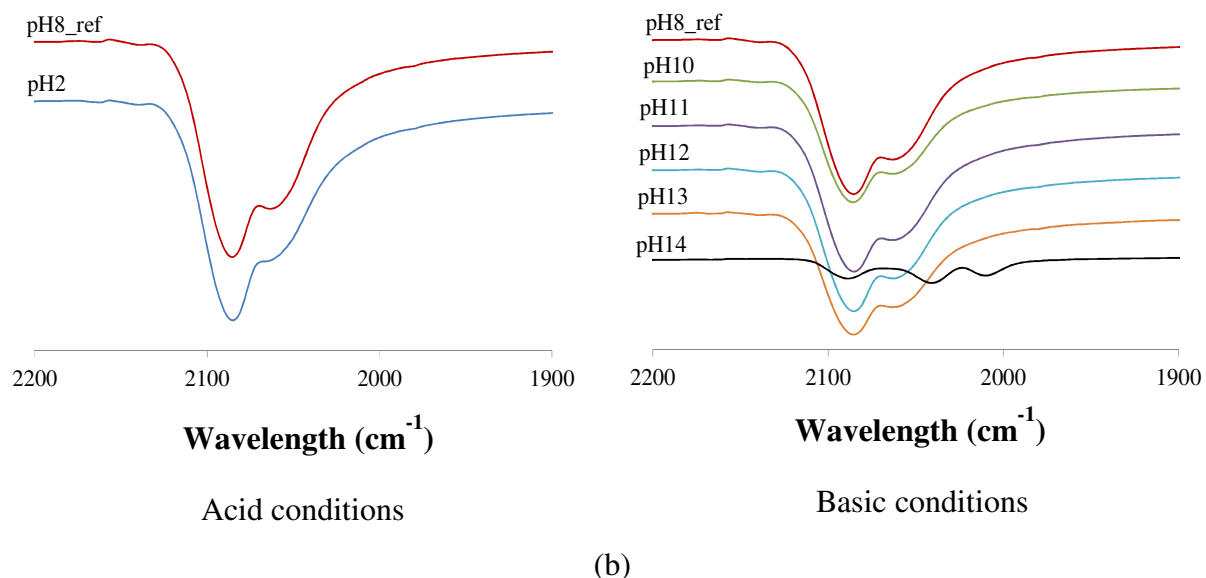


Figure 9: FTIR spectra of Solution I for different pH values of aqueous solution (a) and zooming a section of FTIR spectra around bonding vibrations of KNiFCN products (b).

The lattice parameter of KNiFCN sample with Cs (Solution I – 0.3 mM of Cs) realized after different chemical treatment are presented in the Figure 10 (b). In acid condition (from pH 8 to pH 2), the ‘a’ value is in the same range of the reference sample (pH8_ref), which is in accordance with FTIR analysis (Figure 9). In basic condition (8 to a greater pH transition by addition of NaOH solution), the ‘a’ value was in the range of 10.044 to 10.065. The presence of Cs seems to create an important structural modification of KNiFCN-Cs sample according to the pH of the solution. Infact, when the solution increases from:

- 8 to 10: the ‘a’ value increase from 10.055 to 10.065. This increase is in accordance to the FTIR observations (Figure 9).
- 8 to 11: the ‘a’ value decreases from 10.055 to 10.044. The lack of Cs in solution (Figure 4) seems to indicate that this decrease is not due to the Cs desorption.
- 8 to 12: the ‘a’ value is in the same range of the reference sample (pH8_ref)
- 12 to 13: a decrease of the ‘a’ value is correlated to the decrease in the intensities of ferrocyanure’s vibration (Figure 9) and to the presence of Cs in solution (Figure 4).

The absence of a X-ray diffractogram at pH equal 14 is due to a lack of material to ensure a correct measurement.

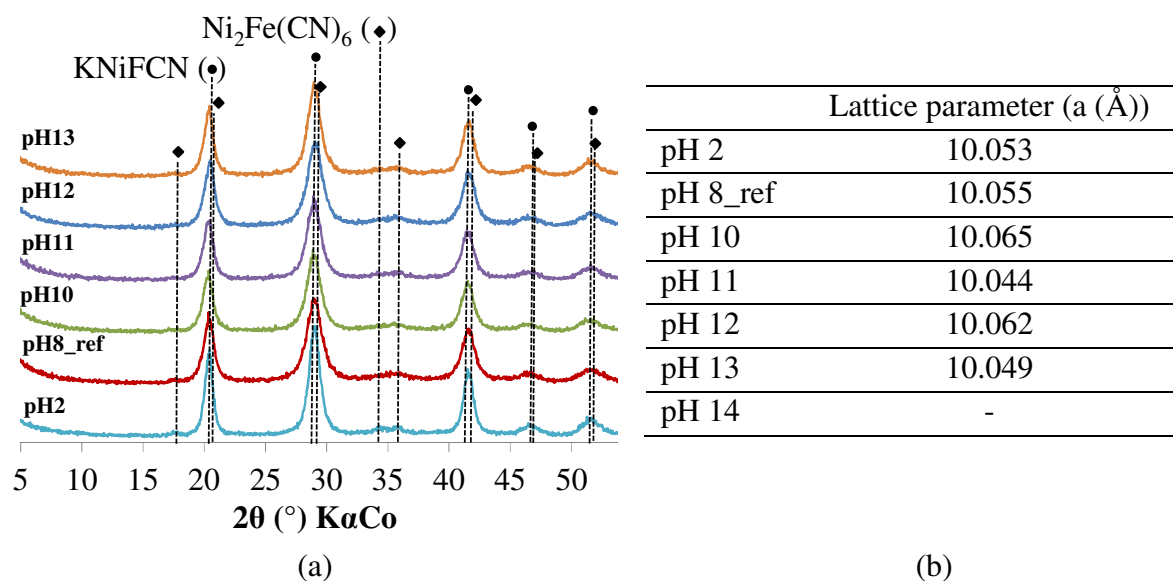


Figure 10: XRD analyses of the Solution I (0.3 mM of Cs) after different chemical treatment (a) and lattice parameter according to the pH values of the aqueous solution (b).

(c) Solution II (30 mM of Cs)

In the case of Solution II (30 mM of Cs), the analysis of the FTIR spectra (presented in Figure 11) revealed the residual presence of ferrocyanure (characteristic band around 2088 cm^{-1}) for the entire pH range tested. Also, this analysis showed the precipitation of one or more new compounds (1483 cm^{-1} , 1392 cm^{-1} and 1241 cm^{-1}) when the pH of the solution is higher than 12 (see orange and black curves). This observations seems to be in adequation with XRD analysis realised in addition (Figure 12 (a)). In fact, following the increase in the pH of the solution, a progressive offset of the characteristics X-ray diffraction lines of $KNiFCN$ is observed. It thus appears that a strong $NaOH$ concentration in the solution leads to a structural ferrocyanure modification due to a possible Na^+ insertion in the ferrocyanure structure [2], [22], [23], or even the precipitation of new compounds such as $Cs_2NiFe(CN)_6$ (represented by triangles) and $KNiFe(CN)_6$ (represented by squares). The precipitation of these new compounds least soluble seems to preserve the conservation of the Cs sorption capacity in the solid phase (0% of Cs detected in solution, see Figure 4).

The FTIR analysis (Figure 11 (b)) and XRD (Figure 12 (a)) also show that in acid condition (Figure 11 (b) (left spectrum)), ferrocyanure is observed. In basic condition (8 to a greater pH transition by addition of $NaOH$ solution, Figure 11 (b) (right spectrum)), the chemical environment of ferrocyanure compounds does not seem to be affected (lack of vibrations bands offset) until pH of solution equal to 12. Beyond pH equal to 12, the vibration intensity

of the ferrocyanure randomly varies, indicating a dissolution/precipitation phenomena of this compound (Figure 11 (b) (right spectrums)). The dissolution/precipitation of the ferrocyanure ensure a trapping of Cs until a pH solution equal 14 (see Figure 4).

As mentioned above, the modification of the pH of the solution leads to the lattice parameter modification of the KNiFCN-Cs sample (Figure 12 (b)).

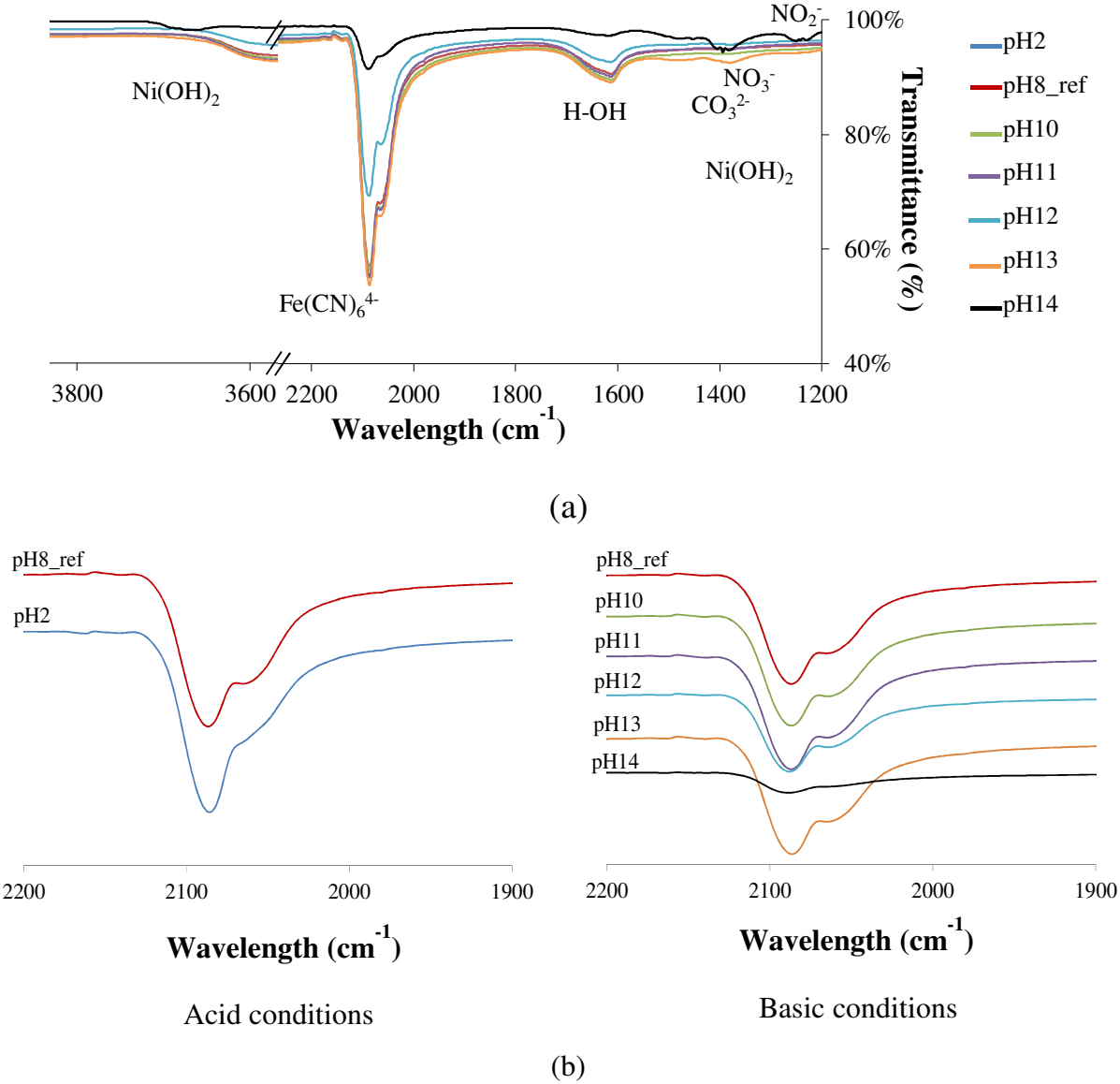


Figure 11: FTIR spectra of Solution II (30 mM of Cs) for different pH values of aqueous solution (a) and zooming a section of FTIR spectra around bonding vibrations of KNiFCN products (b).

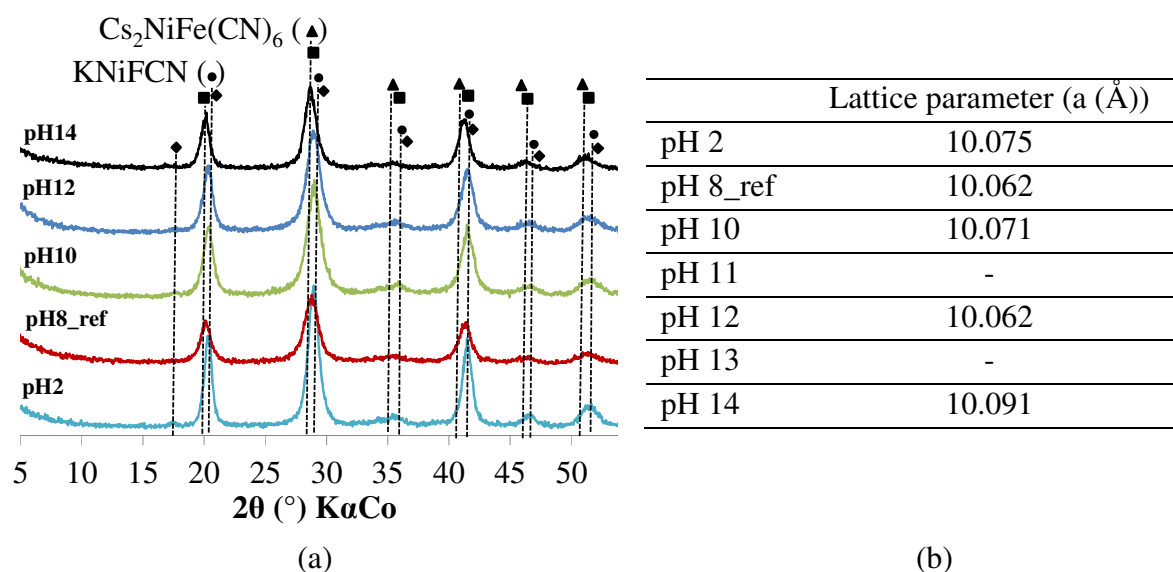


Figure 12: XRD analyses of the Solution II (30 mM of Cs) after different chemical treatment (a) and lattice parameter according to the pH values of the aqueous solution (b).

(d) Solution III (2000 mM of Cs)

The desorption study of Cs in the Solution III (2000 mM of Cs) (see Figure 4) indicates a large variation in the Cs proportions detected in the solution, suggesting a dissolution/precipitation of the new compounds formed from Cs^+ ions and $KNiFCN$ product, according to the alkalinity of the solution. Further analyses realized by FTIR (Figure 13 (a) and (b)) and XRD (Figure 14 (a)) allows monitoring the dissolution/precipitation of the products present in the solid residue, obtained after filtration of the solution. Thus, in acid condition (Figure 13 (b) (left spectrums)), the absence of Cs in the solution seems to be due to the maintenance of ferrocyanure in the solid residue. On another hand, in basic condition (Figure 13 (b) (right spectrums)), changes in intensity of vibration and X-ray diffractions lines of ferrocyanure, according to the pH of the solution, suggest the precipitation of a compound that has a chemical environment identical to ferrocyanures at pH equal to 11 (violet curve). For the whole pH range tested (excluding pH 11 and 14), it appears that the degradation of the ferrocyanures is relatively small, which may explain the low Cs content shown in Figure 4. When the pH of the medium is equivalent to 14, less degradation of the ferrocyanides compared with the previous solutions studied is observed. Similarly, with the exception of the previous solutions, this degradation seems to generate only the formation of iron hydroxide in a small proportion (only detected by XRD, notation N Figure 14 (a)). The lattice parameter show in Figure 14 (b) is in accordance with the previous observations. In fact, the “a” value of

the different sample is in the range of 10.167 to 10.209, which is close to that for original sample (pH8_ref). The most important value is observed for the pH=14, that corresponds to the structural modification do to a possible KNiFCN-Cs products degradation.

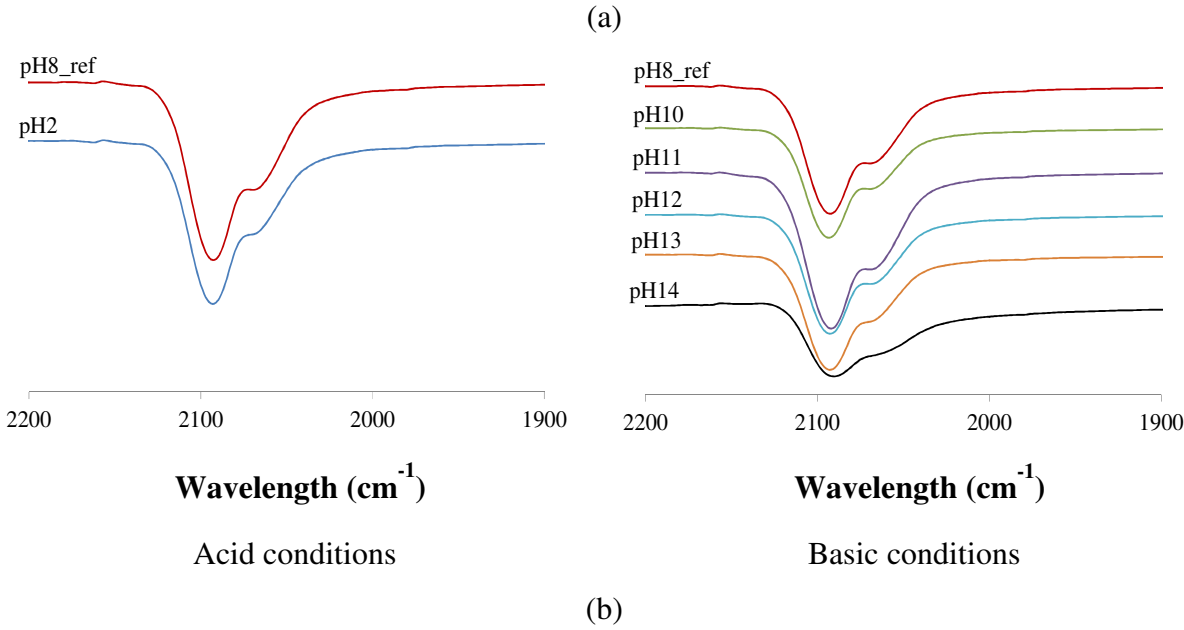
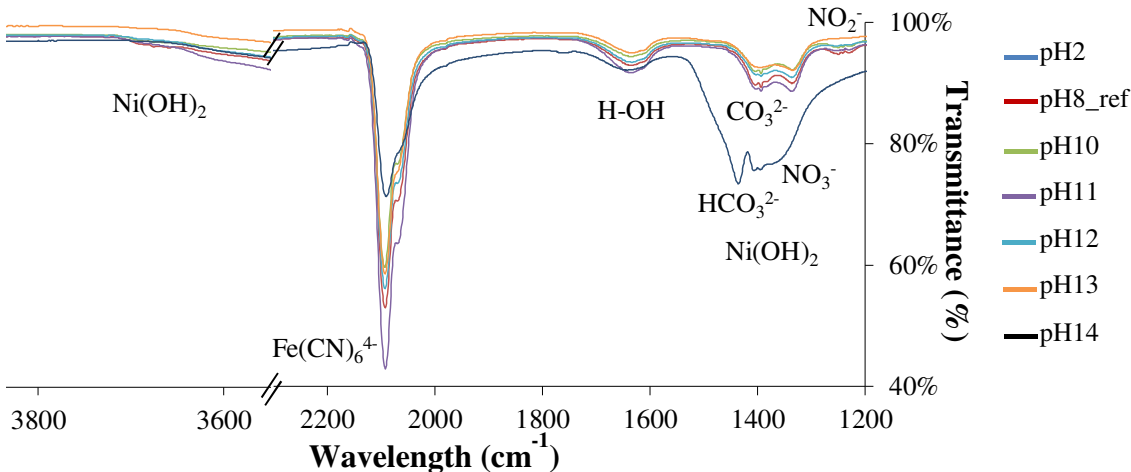


Figure 13: FTIR spectra of Solution III (2000 mM of Cs) for different pH values of aqueous solution (a) and zooming a section of FTIR spectra around bonding vibrations of KNiFCN products (b).

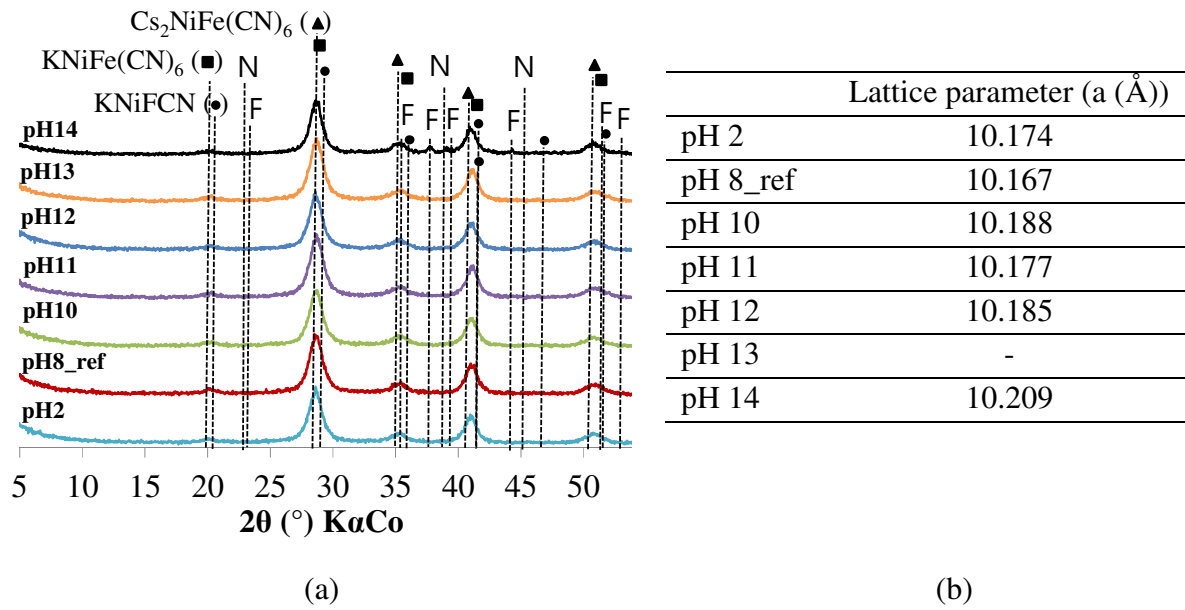


Figure 14: XRD analyses of the Solution III (2000 mM of Cs) after different chemical treatment (a) and lattice parameter according to the pH values of the aqueous solution (b).

3.3 Discussion

3.3.1 Sorption of Cs

Previous studies have made it possible to determine the retention capacity of Cs in hexacyanoferrates ([2], [5], [11], [23]). The distribution coefficient (noted K_d) for Cs leads to determine the selectivity of hexacyanoferrates using the following equation [5]:

$$K_d = \left[\frac{(C_o - C_f)}{C_f} \right] \times \frac{V}{M} \quad (2)$$

where C_o is the initial concentration of Cs (mg/L), C_f is the equilibrium concentration of Cs (mg/L), V is the volume of the testing solution (ml), and M is the amount of $KNiFCN$ present in solution (g). Table 4 illustrates the effects of initials concentrations of Cs on the distribution coefficient (K_d) of Cs^+ . The distribution coefficients (K_d) for Cs were comprise between 2 000 ml/g and 17 000 ml/g for 0.3 mM (Solution I) and 30 mM (Solution II), respectively, which is in accordance with a results observed for loaded chabazites ([24]). For a high concentration of Cs (2000 mM – Solution III), the distribution coefficient decrease to reach the value of 100 ml/g, without causing degradation of sorption capacity of the $KNiFCN$ -Cs product, as observed on Figure 13 and Figure 14.

Table 4: The distribution coefficient (K_d) for Cs for different solutions at pH=8.

Sample	C _o (mg/l)	C _f (mg/l)	K _d (ml/g)
Solution I	3.4	4.9.10 ⁻²	0.2.10 ⁴
Solution II	2.7.10 ²	6.3.10 ⁻¹	1.7.10 ⁴
Solution III	1.6.10 ⁴	1.3.10 ⁴	0.1.10 ²

V (ml) = 100 and 1.8 < M (g) < 2.5

The structure effect of KNiFCN compound is similar with zeolites. Therefore, the selectivity for monovalent cation could be explained by the “sieve” effect [10], [15]. Čeranić [15] determined the effective radii of the “cages” (8 cages per unit cell and their entrances. One of the most important result was the evaluation of the effective radii of the windows of KNiFCN, estimated to be about 0.15 nm, according to equation 3.

$$r_w = \left(\frac{a}{2}\right) - 2r_{e,CN} \quad (3)$$

where *a* is the lattice parameter and *r_{e,CN}* is an equatorial radius (*r_{e,CN}* = 0,178 nm ([25])). Therefore it appears that the effective radii of those windows (*r_w*) depend on the lattice parameter of the system. Table 5 presents the effective radii of the windows of KNiFCN-Cs as fonction of the initial concentrations of Cs in the solution. The increase of the initial concentration of Cs does not lead to a significant increase in *r_w* value, which suggests that the modification of selectivity effect of KNiFCN for Cs⁺ is not only due to the “ion sieve” effect.

Table 5: Effective radii of cell in the KNiFCN solution at pH equal 8.

Sample	a (Å)	r _w (nm)
0.3 mM pH8_reference	10.055	0.147
30 mM pH8_reference	10.062	0.147
2000 mM pH8_reference	10.167	0.152

The analyses conducted on the solid phase (Figure 14) show the presence of new Cs-based compounds, for example Cs₂NiFe(CN)₆. Therefore, it seems that the presence of a high initial concentration of Cs leads to a possible precipitation of KNiFCN-Cs products, probably less soluble at the surface of grains of KNiFCN. It could also occur that Cs is trapped by occupancy of vacants KNiFCN sites.

Figure 15 illustrates the effects of the pH of the solution on the distribution coefficient (K_d) of Cs^+ for the different initial concentration of caesium.

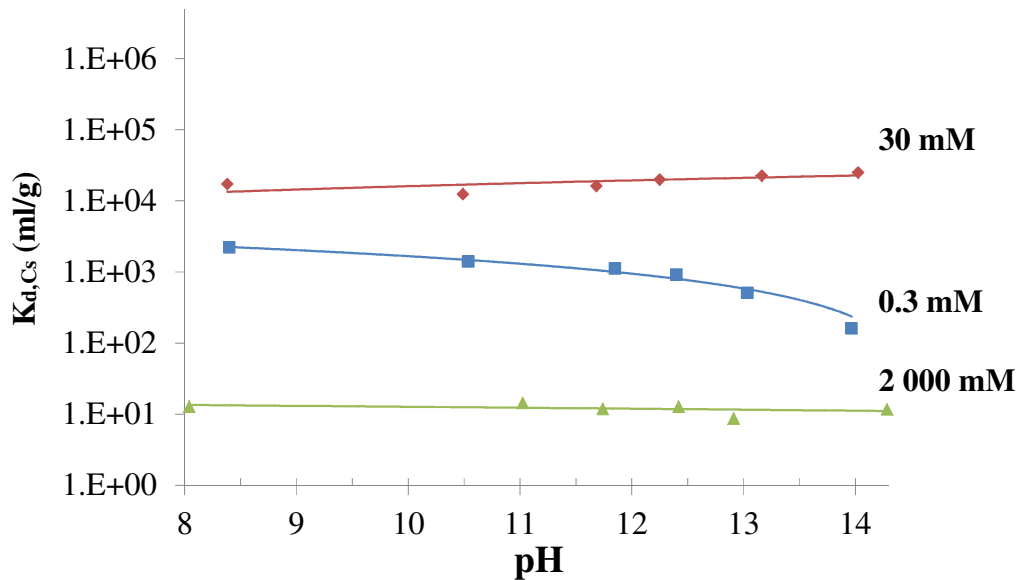


Figure 15: Effects of pH solution on distribution of Cs^+

The K_d value of Cs^+ for the solution varies as a function of the Cs concentration. Two different types of behaviour are observed:

Solution I (0.3 mM of Cs): the K_d value of Cs^+ for KNiFC tends to decrease with the increase of pH of the solution, corresponding to the KNiFCN decomposition.

Solution II (30 mM of Cs) and Solution III (2 000 mM of Cs): the K_d value is almost constantly about 1.10^1 ml/g for 2 000 mM (Solution III) and 1.10^4 ml/g for 0.3 mM (Solution II) over the range of pH.

3.3.2 Stability area and approach on conditioning of the wastes

The influence of the pH of the solution on the KNiFCN and KNiFCN-Cs stability is synthesized into the Figure 16. The light green area correspond to the domain in which the KNiFCN/KNiFCN-Cs is not degraded. In contrast, the orange et red area correspond to the degradation domain of KNiFCN/KNiFCN-Cs products. In the case that any Cs is not present in solution, the KNiFCN stability range is comprise between pH equal to 8 and 12. Beyond this range a significant deterioration, with nickel and iron hydroxide precipitation, is observed. When adding a very low quantity of Cs in the solution (0.3 mM of Cs –Solution I),

it is noted the same stability range as function of pH. The stability range seems to increase with the increase of Cs concentration in the solution. Thus when the Cs concentration is higher than 30 mmol/mmol de Fe (Solution II), KNiFCN-Cs products is detected even at pH equal to or above 13.

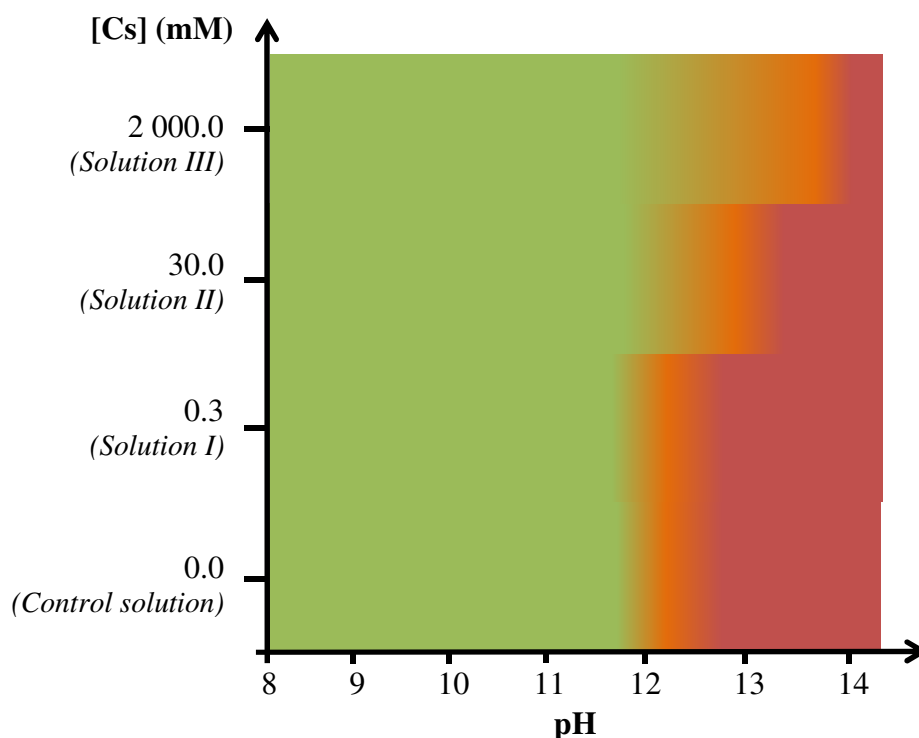


Figure 16: Overview of the KNiFCN and KNiFCN-Cs stability study.

This work aimed to determine the stability range of KNiFCN as function of the pH of the solution in order to contain it in a solid matrix for long term storage. Table 6 resumes the low-pH classical cement composed with a mixed between CEM I and mineral addition like SF, FA and S[†]. The ettringite-based systems are also presented in this table. With the exception of some formulations, all binary or ternary cement are conform with the pH stability range previously defined. It should also be noted the compliance of the ettringite-based systems, making a potential candidate for this specific application.

Table 6: Low-pH cement summary; CEM I: Portland Cement; SF:Silica fume; CAC: Calcium Alunminate Cement; HH:Hemihydrate; FA: Fly Ash; S: Slag (adapted from [26])

[†] FS: Silica Fume, CV: Fly Ash and L: Blast Furnace Slag

Cement	Composition	pH	Measurement conditions	Reference
Binary cement CEM I/SF	CEM I 70% SF 30%	12.2	Days of hydration = 180 w/s = 0.55	[27]
	CEM I 60% SF 40%	11.7	Days of hydration = 360 w/s = 0.55	[27]
		12.2	Days of hydration = 90 w/s = 0.50	[28]
		11.0	Days of hydration = 58	[29]
		11.3	Days of hydration = 360	[30]
	CEM I 50% SF 50%	10.6	Days of hydration = 90 w/s = 1.00	[31]
Binary cement CAC/HH (ettringite systems)	CAC 60% HH 40%	12.0	Days of hydration = 7 w/s = 0.60	[32]
	CAC 50% HH 50%	10.5	Days of hydration = 7 w/s = 0.60	[32]
Ternary cement CEM I/SF/FA	CEM I 37.5% SF 32.5% FA 30%	11.1	Days of hydration = 360 w/s = 0.55	[27]
		11.4	Days of hydration = 360 w/s = 0.40	[33]
	CEM I 35% SF 35% FA 35%	10.9	Days of hydration = 90 w/s = 0.50	[28]
	CEM I 40% SF 20% FA 40%	11.0	Days of hydration = 28 w/s = 0.40	[34; 35]
Ternary cement CEM I/SF/S	CEM I 20% SF 32.5% S 42.5%	11.6	Days of hydration = 360 w/s = 0.55	[27]
	CEM I 37.5% SF 31% S 31.5%	11.6	Days of hydration = 180 w/s = 0.55	[27]
	CEM I 90% Nano silica 10%	12.3	Days of hydration = 360 w/s = 1.10	[27]
Ternary cement CAC/HH/S (ettringite systems)	CAC 52% HH 33% S 15%	10.0	Days of hydration = 7 w/s = 0.60	[36]
Quaternary cement CEM I/SF/FA/S	CEM I 33% SF 40% FA 13.5% S 13.5%	12.1	Days of hydration = 360 w/s = 0.50	[37]
	CEM I 40% SF 5% FA 25% S 30%	12.7	-	[38]

4 Conclusions

The investigation of Cs retention properties in KNiFCN, according to the pH of the solution, has put forward many aspects. Thus, it was found that the increase in Cs sorbed changed the structure of KNiFCN products, influencing the Cs sorption capacity as function of pH. In fact, without Cs sorbed (Control Solution), the pH range on which KNiFCN is stable is comprised between 8 and 12. When a low amount of Cs is sorbed (Solution I), the pH range in which the Cs remains trapped is slightly similar to the control solution. Thereafter, when the concentration of Cs is increased (Solution II), the lack of variations in Cs proportions on the

whole pH range seems to indicate that Cs remains trapped in the solid phase, over a higher pH range ($8 < \text{pH} < 13$). Finally, in cases where the concentration of Cs sorbed is maximum (Solution III), ferrocyanures remains detected at pH equal 14.

Further analyses were carried out by XRD, SEM-BSE and FTIR in order to determine the degradation products of the KNiFCN-Cs systems according to the pH values of the aqueous solution. First of all, the chemical composition obtained by SEM-BSE confirmed that the principal Cs sorption capacity into the KNiFCN structure is made by the K^+ ions replacement. However, it has been found that all of these ions are not substitutable. Despite a higher Cs concentration in the solution, potassium remains in the crystal structure of KNiFCN and the excess Cs precipitates into new compounds on the surface of KNiFCN. Similarly, the results on microstructural evolution as function of the pH of the solution show that the alkalinity and the Cs content sorbed have an impact on the ferrocyanures compositions:

- In acid condition, no changes were observed on chemical environment of the ferrocyanure compounds and no new compound was detected.
- In basic condition, under certain conditions, a change of chemical environment of the ferrocyanure compounds was observed. Furthermore, a dissolution/precipitation of new compounds resulting from KNiFCN-Cs products downgrading, such as nickel and/or iron hydroxide ($\text{Ni}(\text{OH})_2$, $\text{Fe}(\text{OH})_2$ and/or $\text{Fe}(\text{OH})_3 \cdot (\text{H}_2\text{O})$), was shown.

The observations carried out during this project have put on evidence that the increase in amount of Cs sorbed leads to the precipitation of new compounds based on KNiFCN and Cs. This precipitation is particularly present in cases where Cs concentration is maximum (Solution III). Similarly, the presence of ferrocyanure and the lack of hydroxide confirm that the increase in Cs concentration stabilized the KNiFCN-Cs products until a strong pH values (pH equal 2 and 14) while forming a low soluble compounds such as $\text{Cs}_2\text{NiFe}(\text{CN})_6$.

In order to ensure the sludge conditioning for nuclear process by avoiding the discharge of Cs entrapped in the KNiFCN structure, the cementing system developed hereafter will have to satisfy pHs below 12. Binary and ternary ettringite based systems could be potentially good candidates for such applications.

Acknowledgements

The authors wish to thank Orano Projets for fundings and especially D. Avril (Orano Projets) for the provision of KNiFCN products and his valuable suggestions and discussions on this work.

Data availability

The raw/processed data required to reproduce these findings cannot be shared at this time as the data also forms part of an ongoing study.

References

- [1] Y. Takahatake, S. Watanabe, A. Shibata, K. Nomura, and Y. Koma, "Decontamination of Radioactive Liquid Waste with Hexacyanoferrate(II)," *Procedia Chem.*, vol. 7, pp. 610–615, Jan. 2012.
- [2] H. Mimura, J. Lehto, and R. Harjula, "Selective Removal of Cesium from Simulated High-level Liquid Wastes by Insoluble Ferrocyanides," *J. Nucl. Sci. Technol.*, vol. 34, no. 6, pp. 607–609, 1997.
- [3] D. Ding, Y. Zhao, S. Yang, W. Shi, Z. Zhang, Z. Lei, and Y. Yang, "Adsorption of cesium from aqueous solution using agricultural residue - Walnut shell: Equilibrium, kinetic and thermodynamic modeling studies," *Water Res.*, vol. 47, no. 7, pp. 2563–2571, 2013.
- [4] W. E. Prout, E. R. Russell, and H. J. Groh, "Ion exchange absorption of cesium by potassium hexacyanocobalt (II) ferrate (II)," *J. Inorg. Nucl. Chem.*, vol. 27, pp. 473–479, 1965.
- [5] C.-Y. Chang, L.-K. Chau, W.-P. Hu, C.-Y. Wang, and J.-H. Liao, "Nickel hexacyanoferrate multilayers on functionalized mesoporous silica supports for selective sorption and sensing of cesium," *Microporous Mesoporous Mater.*, vol. 109, no. 1–3, pp. 505–512, Mar. 2008.
- [6] K. Shakir, M. Sohsah, and M. Soliman, "Removal of cesium from aqueous solutions and radioactive waste simulants by coprecipitate flotation," *Sep. Purif. Technol.*, vol. 54, no. 3, pp. 373–381, 2007.
- [7] IAEA, "Radioactive Waste Management," no. February. pp. 1–191, 2005.
- [8] H. Mimura, J. Lehto, and R. Harjula, "Ion Exchange of Cesium on Potassium Nickel," *J. Nucl. Sci. Technol.*, vol. 34, no. 5, pp. 484–489, 1997.
- [9] IAEA, "Treatment of Low and Intermediate Level Liquid Radioactive Wastes," *Technical Report Series n°236*, Vienna, 1984.
- [10] H. Mimura, J. Lehto, and R. Harjula, "Chemical and thermal stability of potassium nickel hexacyanoferrate(II)," *J. Nucl. Sci. Technol.*, vol. 34, no. 6, pp. 582–587, 1997.
- [11] H. Mimura, J. Lehto, and R. Harjula, "Chemical and Thermal Stability of Potassium Nickel Hexacyanoferrate (II)," *J. Nucl. Sci. Technol.*, vol. 34, no. 6, pp. 582–587, Jun. 1997.
- [12] C. Ravat and V. Tessier, "Etude des interactions radionucléides/sels peu solubles du procédé STE3," *CEA/DEN/DED*, vol. Note techn, 2000.
- [13] P. A. Haas, "A Review of information on ferrocyanide solids for removal cesium from solutions," *Sep. Sci. Technol.*, vol. 28, no. 17–18, pp. 2479–2506, 1993.
- [14] P. Gellings, "Structure of some Hexacyanoferrates (II) of the Type $K_2MIIFe(CN)_6$," *Zeitschrift für Physikalische Chemie*, vol. 54. p. 296, 1967.

- [15] T. Čeranić, “The Structure Model of an Inorganic Ion Exchanger Cobalt (II) - hexacyanoferrate (II),” vol. 1488, no. Ii, pp. 1484–1488, 1978.
- [16] M. M. K. Motlagh, a a Youzbashi, and L. Sabaghzadeh, “Synthesis and characterization of Nickel hydroxide / oxide nanoparticles by the complexation-precipitation method,” *Int. J. Phys. Sci.*, vol. 6, no. 6, pp. 1471–1476, 2011.
- [17] C. Loos-Neskovic, S. Ayrault, V. Badillo, B. Jimenez, E. Garnier, M. Fedoroff, D. . Jones, and B. Merinov, “Structure of copper-potassium hexacyanoferrate (II) and sorption mechanisms of cesium,” *J. Solid State Chem.*, vol. 177, no. 6, pp. 1817–1828, Jun. 2004.
- [18] T. Richard, L. Mercury, F. Poulet, and L. d’Hendecourt, “Diffuse reflectance infrared Fourier transform spectroscopy as a tool to characterise water in adsorption/confinement situations,” *J. Colloid Interface Sci.*, vol. 304, no. 1, pp. 125–136, 2006.
- [19] A. S. Adekunle, J. A. O. Oyekunle, O. S. Oluwafemi, A. O. Joshua, W. O. Makinde, A. O. Ogunfowokan, M. A. Eleruja, and E. E. Ebenso, “Comparative catalytic properties of Ni(OH)₂ and NiO nanoparticles towards the degradation of nitrite (NO₂⁻) and nitric oxide (NO),” *Int. J. Electrochem. Sci.*, vol. 9, no. 6, pp. 3008–3021, 2014.
- [20] S. Ayrault, B. Jimenez, E. Garnier, M. Fedoroff, D. . Jones, and C. Loos-Neskovic, “Sorption Mechanisms of Cesium on Cu_{II}2Fe_{II}(CN)₆ and Cu_{II}3[Fe_{III}(CN)₆]₂ Hexacyanoferrates and Their Relation to the Crystalline Structure,” *J. Solid State Chem.*, vol. 141, no. 2, pp. 475–485, Dec. 1998.
- [21] R. Chen, H. Tanaka, T. Kawamoto, M. Asai, C. Fukushima, H. Na, M. Kurihara, M. Watanabe, M. Arisaka, and T. Nankawa, “Selective removal of cesium ions from wastewater using copper hexacyanoferrate nanofilms in an electrochemical system,” *Electrochim. Acta*, vol. 87, pp. 119–125, Jan. 2013.
- [22] R. Martínez-García, E. Reguera, J. Balmaseda, G. Ramos, and H. Yee-Madeira, “On the crystal structures of some nickel hexacyanoferrates (II,III),” *Powder Diffr.*, vol. 19, no. 3, pp. 284–291, 2004.
- [23] H. Mimura, M. Kimura, and K. Akiba, “Selective Removal of Cesium from Sodium Nitrate Solutions by Potassium Nickel Hexacyanoferrate-Loaded Chabazites,” *Sep. Sci. Technol.*, vol. 34, no. 1, pp. 17–28, 1999.
- [24] H. Mimura, M. Kimura, K. Akiba, and Y. Onodera, “Separation of Cesium and Strontium by Potassium Nickel Hexacyanoferrate(II)-loaded Zeolite A,” *J. Nucl. Sci. Technol.*, vol. 36, no. 3, pp. 307–310, 1999.
- [25] J. A. Lely and J. M. Bijvoet, “The crystal structure of lithium cyanide,” *Recl. des Trav. Chim. des Pays-Bas*, vol. 61, no. 4, pp. 244–252, 1942.
- [26] T. Leung, Les bétons bas pH: comportements initial et différé sous contraintes externes, PhD thesis, Université de Toulouse, France, 2015
- [27] T.T.H, Bach, "Evolution physico-chimique des liants bas pH hydrates - Influence de la température et mécanisme de rétention des alcalins“, PhD thesis, Université de Bourgogne, France, 2010
- [28] J.L. García Calvo, M.C. Alonso, A. Hidalgo, L. Fernández-Luco, “Design of low-pH cementitious materials based on functional requirements”, Proceeding 3rd workshop R&D on low pH cement for a geological repository, Paris, 2007, pp.48-51.

- [29] U. Vuorinen, J. Lehtikoinen, Low pH grouting cements - Results of leaching experiments and Modelling, Proceeding 2nd workshop R&D on low pH cement for a geological repository, Madrid, Spain, 2007.
- [30] T. Fries, H. Weber, V. Wetzig, "Low pH shotcrete field tests on opalinus clay samples", Proceeding 3rd workshop R&D on low pH cement for a geological repository, Paris, France, 2007, pp.107-115.
- [31] J.B. Martino, "Low heat high performance concrete used in a full scale tunnel seal", Proceeding 3rd workshop R&D on low pH cement for a geological repository, Paris, 2007, pp.89-97.
- [32] I. Martin, C. Patapy, M. Cyr, "Impact of calcium sulfate type and additions on hydration and properties of ettringite-based systems", Proceedings ICCG congress, Pekin, Chine, 2015
- [33] A. Dauzère, "Étude expérimentale et modélisation des mécanismes physico-chimiques des interactions béton-argile dans le contexte du stockage géologique des déchets radioactifs", PhD thesis, Université de Poitiers, 249 p.
- [34] T. Nishiuchi, T. Yamamoto, M. Hironaga, H. Ueda, Mechanical properties of low pH concretes, LAC, HFSC and SAC", Proceeding 3rd workshop R&D on low pH cement for a geological repository, Paris, 2007, pp.62-71.
- [35] Y. Kobayashi, T. Yamada, H. Matsui, M. Nakayama, M. Mihara, M. Naito, M. Yui, "Development of low-alkali cement for application in a JAEA URL", Proceeding 3rd workshop R&D on low pH cement for a geological repository, Paris, France, 2007, p. 98-106
- [36] I. Martin, C. Patapy, M. Cyr, "Parametric study of binary and ternary ettringite-based systems", Proceedings CAC 2014, ISBN ?, HIS Bre Press, Avignon, France, 2014
- [37] M. Codina M, "Les bétons bas pH: formulation, caractérisation et étude à long terme", PhD thesis, Université Toulouse III - Paul Sabatier, Laboratoire Matériaux et Durabilité des Constructions, Toulouse.
- [38] L.R. Dole, C.H. Mattus, "Low pH concrete for use in the US high level waste repository: Part 1 Overview", Proceeding 2nd workshop R&D on low pH cement for a geological repository, Madrid, Spain, 2007.
- [39] H. El-Didamony, A.A. Amer, H.A. Ela-ziz "Properties and durability of alkali-activated slag pastes immersed in sea water", *Ceramics International*, vol. 38, no 5, pp. 3773-3780, 2012.
- [40] A. Miller, C.H. Wilkins "Infrared Spectra and Characteristic Frequencies of inorganic Ions - Their Use in Qualitative Analysis", Departement of Research in Chemicals Physics, Mellon Institute, Pittsburg 13, Pa.

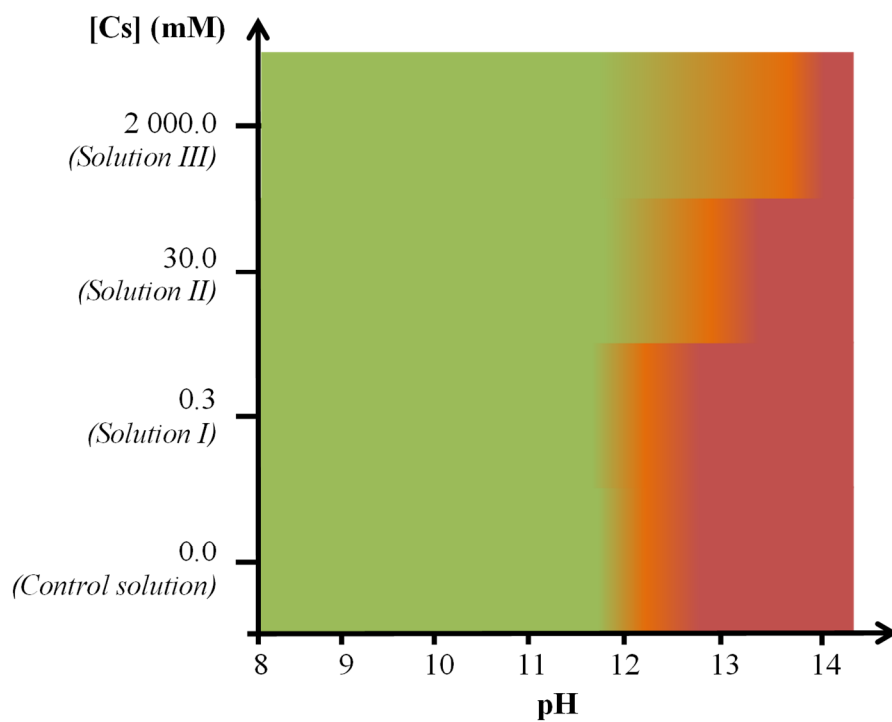


Figure 1: Overview of the KNiFCN and KNiFCN-Cs stability study as a function of pH.